Academic Journal of Science and Technology
ISSN: 2771-3032 | Vol. 20, No. 1, 2026

Research on Non-destructive Testing Technology for Bolt Deformation based on Stress Wave Method

Jie Zhang [1, a], Hu Li [2, b]

[1] Shaanxi Shanmei Hancheng Mining Co., Ltd., Hancheng, Shaanxi, 715400, China
[2] School of Mining Engineering, Anhui University of Science and Technology, Huainan, Anhui, 232001, China
[a] 1691857577@qq.com, [b] lihu18255113623@126.com

Abstract: In response to the difficulty that bolts are prone to large deformation failure in support and cannot be accurately detected for defects, a comprehensive approach is employed, integrating laboratory experiments, numerical simulation, and experimental validation to study the non-destructive testing method of bolt deformation. The research results demonstrate that: (1) The propagation characteristics of stress waves at varying stages of bolt stretching are elucidated, and it is proposed that the energy decay ratio be employed to quantify the extent of stress wave energy decay at distinct stages of bolt stretching. It is observed that the degree of stress wave energy decay escalates with the degree of stretching. (2) The visualization results of the numerical simulation demonstrate the propagation process of the stress wave at varying stages of bolt stretching with greater clarity, thereby corroborating the stress wave energy decay law at distinct stages of bolt stretching. (3) A non-destructive testing method for bolt deformation is proposed, and the evaluation criteria for non-destructive testing of bolt deformation state are given.

Keywords: Stress-wave Nondestructive Testing; Bolt Stretching; Energy Attenuation Ratio.

1. Introduction

The stability of tunnel surrounding rock is essential for safe and efficient coal mine production [1]. Bolt support is currently the most widely used method for roadway support [2]. During service, bolt stress and deformation directly affect surrounding rock strength and roadway stability. Under large roadway deformation, bolts release surrounding rock pressure through elongation and mainly bear tensile loads, during which they may undergo elastic deformation, plastic deformation, or fracture. Their axial load generally increases first and then decreases. Although axial force monitoring can reflect the support state of bolts, it cannot distinguish whether a low axial force corresponds to elastic deformation or plastic deformation [3,4].

Previous studies have investigated the plastic deformation and structural damage of metal bolts during tension. Salita D. S. et al. [5] found that alloying element content influences acoustic emission characteristics in Pb-Sn alloys under static loading, and showed that increased β-phase content can suppress dislocation activity during plastic deformation. Ouyang, H. [6] investigated the acoustic emission characteristics of two metal materials during stretching and found strong correlations among ringing counts, amplitude, and energy. Tian, S. [7] revealed the acoustic emission characteristics of high-strength bolts before fracture through uniaxial tensile tests and further used acoustic emission technology to monitor bolt status during fracture tests. These studies indicate that acoustic emission can characterize the deformation process of bolts; however, it remains difficult to identify the deformation state of a bolt at a specific moment.

To overcome this limitation, some scholars have applied stress wave methods to bolt non-destructive testing (NDT). Ivanović, A. et al. [8] evaluated prestressed anchor bolts using magnetostrictive exciters under cyclic loading and suggested that an appropriate excitation frequency should be selected according to the effective bolt length for fracture monitoring. Vrkljan, I. et al. [9] proposed a method for evaluating the anchorage quality of grouted anchor bolts by analyzing the acceleration history and principal frequency changes of axial stress waves. Zhang, J. et al. [10] used signal processing methods to identify defects in GFRP anchorage systems and improve the recognition of defect locations and lengths. Zhang, L. [11] analyzed reconstructed NDT signals using multi-scale entropy and found that defective anchorage systems showed significantly higher entropy values than non-defective systems. Li, C. et al. [12] identified a relationship between bolt axial force and the time-domain amplitude of stress waves during pull-out tests, and proposed a method for axial force detection. Wang, Y. et al. [13] established a model relating bolt vibration frequency to axial force based on contact mechanics theory and proposed a real-time NDT method based on the nonlinear vibration characteristics of bolt components. Wang, M. et al. [14] proposed using wavelet transform to identify the time and location of structural damage from transient vibration differences. Hao, Y. et al. [15] and Wu, F. et al. [16] analyzed the limitations of current bolt NDT in field applications and proposed directions for future development.

Overall, current bolt NDT research mainly focuses on bolt length, anchorage quality, and axial force [8–16]. Although stress wave technology has advantages such as long propagation distance, strong anti-interference ability, convenient operation, and easy miniaturization, NDT methods for bolt deformation remain limited. This restricts the evaluation of bolt deformation state during service, particularly the discrimination between elastic and plastic deformation. Therefore, it is necessary to develop an effective and convenient NDT method for bolt deformation.

This study focuses on support bolts subjected to significant tensile deformation, under which plastic deformation and even fracture may occur. The deformation state of bolts at this stage has received limited attention, especially in NDT research. Therefore, laboratory tests, numerical simulations,

and experimental validation were combined to investigate the stress-wave response characteristics of bolt tensile deformation. The results are expected to provide a basis for deformation-state identification and to extend the application of stress-wave NDT in bolt support systems.

2. Experimental Study on Stress Wave in Bolts at Different Tensile Stages

2.1. Experimental Setup for Rock Bolt Tensile Loading and Stress-Wave Testing

Figure 1 shows the experimental setup used for rock bolt deformation monitoring, which consisted of a rock bolt tensile loading system, a stress-wave testing system, and a rock bolt state monitoring system. The tested rock bolt was a left-handed threaded rock bolt made of 20MnSi steel, with a diameter of 20 mm, a length of 1200 mm, a yield strength of 500 MPa, and an ultimate elongation of 15%. Before testing, the end face of each rock bolt was polished, the outer surface was sprayed with white paint, and visible scale marks were added. These treatments were used to improve observation of deformation development and to facilitate data acquisition during stress-wave testing and rock bolt state monitoring.

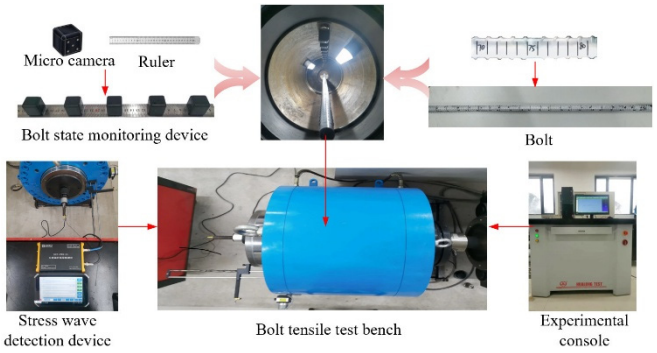

Fig 1. Bolt tension & Stress-Wave detection testing equipment

During the test, axial displacement was applied to the end of the rock bolt through the tensile loading system at a loading rate of 10 mm/min. Stress waves were generated by a roller exciter positioned 10 cm from the end of the rock bolt. Acceleration sensors were installed at the end section of the rock bolt to collect stress-wave response data. Each measurement was repeated six times. In addition, a miniature camera was used to continuously record the tensile deformation process of the rock bolt.

A total of three experimental groups were designed, with three rock bolts in each group.

2.2. Deformation Characteristics and Bolt Strain Analysis

The axial load-deployment curves were plotted based on data finally collected by the experimental system. As shown in Fig. 2, the bolt eventually undergoes ductile fracture under axial displacement loading, which is a normal behavior of steels or alloys. Since the deformation capacity of the bolt varies at different stages, it is necessary to study the data obtained from the experimental collection in stages.

Condition Monitoring System records the process of bolt condition changes throughout the bolt tensioning process. Based on the data recorded, it can be observed that the cross-sectional diameter of a bolt at a given location decreases in size until the bolt neck fracture occurs. The objective is to organize and analyze the rules for diameter changing at the constriction position as various axial displacements are imposed on it. Given that axial displacement within bolt varies at different stages, a new variable, S, is introduced to quantify this variation. S is defined as the ratio of the axial displacement to the total extension, and its calculation formula is as follows:

$$S = \frac{Axial\ displacement}{Total\ extension} \tag{1}$$

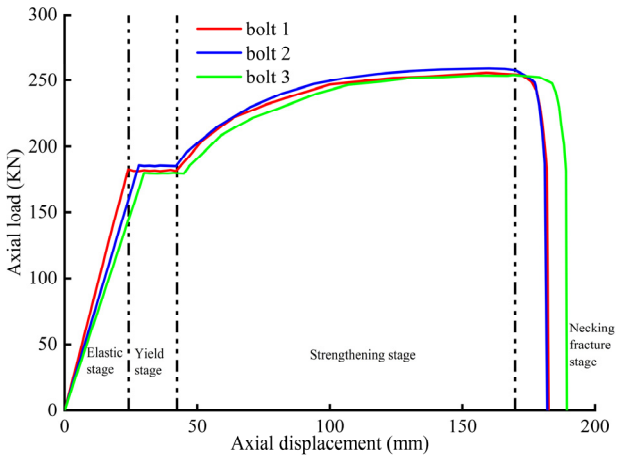

Fig 2. Axial load-displacement curves for each bolt.

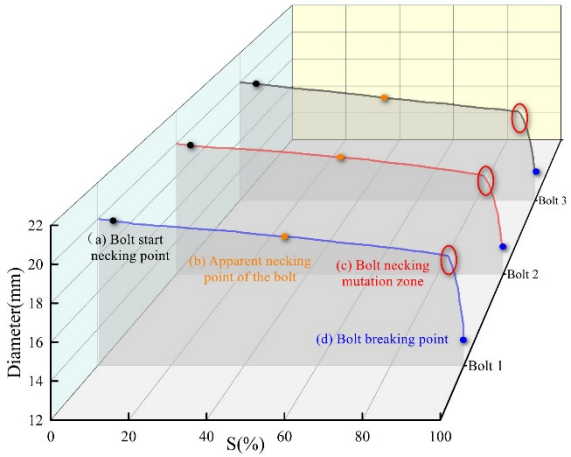

Fig 3. Diameter change versus bolt neck position.

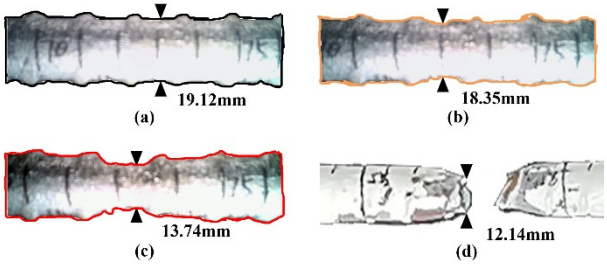

Fig 4. Bolt necking diameter variation graph.

Figures 3 and 4 illustrate the graphs of diameter change at the position of necking down of the bolts and the diameter change of the bolts at the corresponding stages, respectively. From an examination of the graphs, it can be discerned that the bolts with identical parameters exhibited comparable diameter alterations during the necking process. The diameter of the bolts undergoes a gradual change at points (a) and (b). Upon reaching the vicinity of point (c), the diameter of the bolt experiences a sudden and precipitous decline, reaching a minimum of 13.74 mm. This is followed by a rapid necking zone, during which the diameter of the cross-section decreases rapidly until the bolt is completely fractured at point (d), accompanied by ductile metal damage.

2.3. Characteristics and Investigation for Stress Wave Propagation Through Bolt Tensioning

The previous study found that apparent deformation phenomena occurred in the anchor bolt at different stages of tensioning; in order to facilitate the real-time detection of the morphology change process of the anchor bolt, it is proposed to use the stress wave method to monitor the whole process of the anchor bolt tensioning. Figure 4 shows the time domain diagrams of the stress wave detection signals when the bolt is stretched to different stages; the stress wave detection signals of the different stretching stages of the anchor are analyzed after denoising.

As illustrated in Figure 5, the bolt's stress wave amplitude exhibits a declining trend at varying axial displacements. However, attenuation varies at different moments, which can be attributed to the transmittance and reflection phenomena that occur when the stress wave propagates in the medium. This results in the attenuation of energy.

The propagation of stress waves in a medium involves three main types of energy: incident energy, reflected energy, or Decaying energy. As each bolt is in a different stretch state, the Decaying energy is different. Therefore, the energy Decaying ratio, defined as the ratio of Decaying energy to incident energy, is proposed to determine the stretching state of bolts. The energy-decaying ratios for bolts at different stretching stages are shown in Figure 6.

As shown in Fig. 6, the energy decay process during stress wave detection is transformed into an energy decay ratio. It can be observed that the energy decay ratio exhibits considerable variation across different tensile stages. The energy decay ratio shows a linear growth pattern during the elastic and yielding phases. Upon entering the strengthening stage, the energy decay ratio undergoes a long up-and-down oscillation. Upon entering the necking phase, the energy decay ratio transforms, reaching 35% and exhibiting exponential growth. This growth continues until the bolt reaches the point of complete necking and failure. The foregoing analysis shows that energy decay ratios of bolt stress waves can accurately determine bolt elongation stages and effectively infer whether a bolt is necked or not. This can be employed as a metric for assessing the state of bolt stretching.

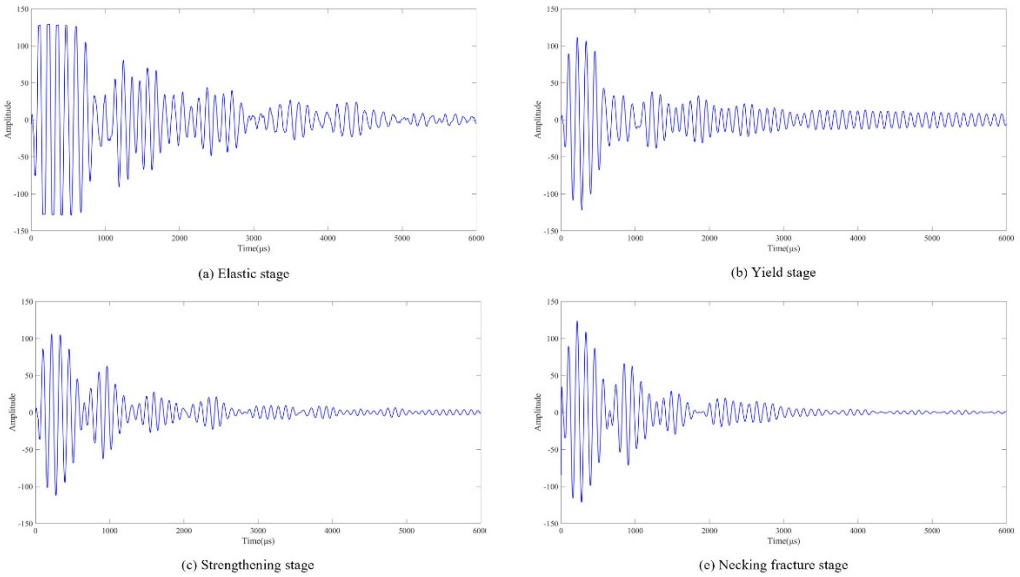

Fig 5. Time domain plot of stress wave detection signatures for bolts in various stretch states.

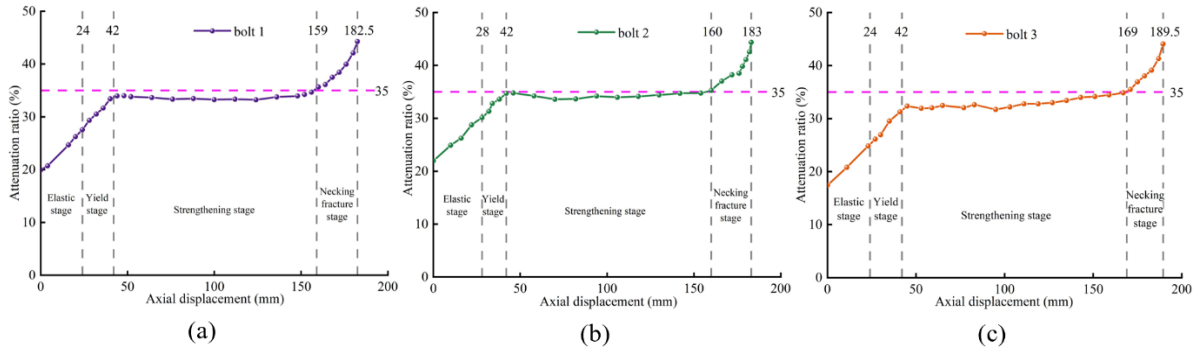

Fig 6. Stress-wave energy variation versus time through bolt stretching.

2.4. Decaying Energy Ratios in Diameter Stress Wave Detection during Bolt Tensioning

The above data show that bolt diameter decreases while stress wave energy decay ratio increases throughout the stretch. This suggests that there may be a correlation along bolt diameter with stress wave energy decay rate within the tensile process. To investigate this further, it is suggested that stress wave energy decay ration be used to determine the diameter of the bolt at neck shrinkage. This would enable a more accurate assessment of the bolt support capacity. Figure 7 illustrates the distribution of data points for each bolt test. A suitable fitting equation can express the relationship between the bolt diameter and the energy attenuation ratio.

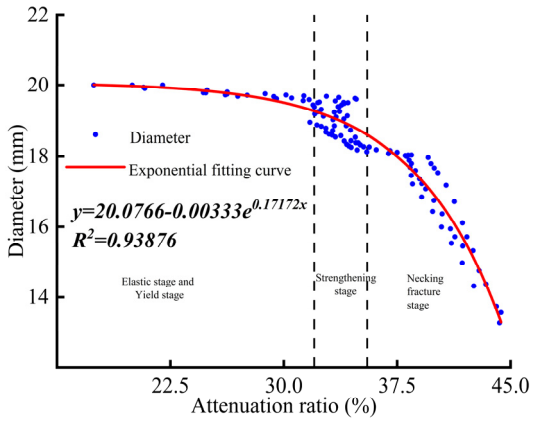

Fig 7. Distribution of test data points for bolt and Exponential function fitting curve.

As illustrated in Figure 7, an increase in the energy attenuation ratio is accompanied by a gradual reduction in the diameter of the bolt, which initially follows a linear trajectory before transitioning to an oscillatory phase and subsequently to an exponential decline. In conjunction with the analysis above, the online elasticity and yielding stages of the bolt diameter remain relatively unchanged, resulting in a relatively minor energy attenuation ratio within the 20% to 33% interval of the rate of change. A further decrease in bolt diameter characterizes the strengthened stage, offset by the energy attenuation ratio oscillating between an up and down period. Consequently, the diameter of the bolt cannot be accurately characterized between the two relationships. Once the necking fracture period is reached, it can be observed that the bolt diameter first passes through a period of stability and then rapidly decreases. This further substantiates the assertion that the necking of the bolt is a crack-expanding process, which aligns with the conventional ductile metal damage process.

The attenuation trend of the data point distribution was compared with the residual analysis using the power function, exponential function, and polynomial function. The exponential function was determined to have the best fitting effect, and the fitting equation along stress wave energy decay relation with bolt diameter was obtained.

3. Numerical Study on Stress Wave Propagation in Bolts at Stretching Stages

3.1. Establishment of Numerical Calculation Models

Simulation stress wave propagations within bolt under NDT using ABAQUS software, the visualization results obtained from the simulation clearly show the attenuation as stress wave in bolt is stretched. Model components include bolt and small hammer used to create vibrations. The dimensions of the bolt and the small hammer are Φ 20 × 1200 mm and Φ 5 × 20 mm. Set up the elastic-plastic constitutive model based on the experimental results., the small hammer and bolt are consistent, with density, elastic modulus, and Poisson's ratio of 7850 kg/m3, 210 Gpa, and 0.3, respectively. Apply axial load to the end face of the bolt on the small hammer side and set fixed constraints on the other end face. The mesh element type selected for bolt material is the hexahedral mesh reduced integral element C3D8R. The bolt mesh size is selected as 2 mm, and the small hammer mesh size is selected as 1 mm.

3.2. Propagation Rule for Stress Wave During Bolt Stretching

Simulation first applies a concentrated force to elongate near center of bolt tail. When the bolt reaches the set time, the small hammer is controlled to impact the center of the bolt end at the initial speed. The small hammer strikes the bolt tail to create stress waves, and then the propagation rule of the corresponding stress waves in the bolt is studied. Extract the global stress cloud maps at different times for stress wave progression within the bolt for analysis. Figures 8 and 9 show stress wave progression of the bolt in unstressed and necked fracture states, respectively.

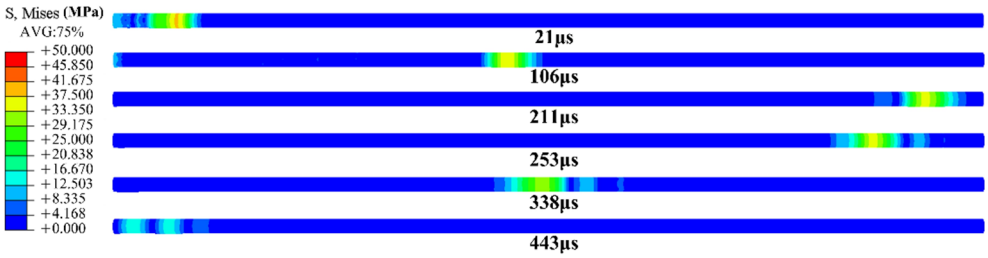

Fig 8. Stress wave propagation process when bolt is not stretched

From Fig. 8, a stress wave generates when the hammer strikes the bolt at 21 μs, and the stress wave propagates along the bolt; The stress wave of the bolt propagates to the middle position of bolt at 106 μs. Stress wave of the bolt propagates to the position close to a right surface of this bolt in 211 μs. At this point, the stress wave has not yet reflected and the bolt has not yet been stretched, it can be seen that the stress attenuation is slow; The stress wave of the bolt propagates to the right end face of the bolt and reflects back at 253 μs. The stress wave from the bolt continues toward the excitation

point along the Z-axis positive direction at 338 μs. The stress wave from the bolt propagates back toward the left end face of the bolt at 443 μs, and the sensor is located at the center of the left end face. At this time, the energy of the stress wave is lost through a reflection and propagation of twice the length of the bolt, and the energy is significantly reduced.

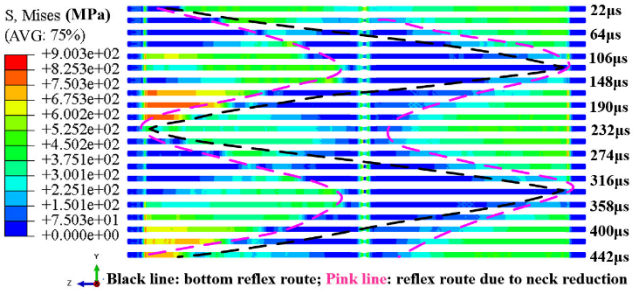

Fig 9. Stress wave propagation process during the necking and fracture stage of bolt

From Fig. 9, it can be seen that when the small hammer strikes the bolt at 22 μs, a stress wave is generated. The bolt body experiences stress in the positive Z-axis directions due to the load originally applied. After the stress wave enters the bolt, it applies stress in the opposite direction to the bolt, which cancels out the stress and reduces the stress at the left end of the bolt. the stress wave of the bolt propagates to the necking position in the middle of the bolt at 64 μs, due to the necking of the bolt, the wave impedance at the necking position of the bolt decreases. At this time, a part of the stress wave reflects and propagates back along the positive Z-axis direction (as shown by the pink line in the figure), while another part continues to propagate along the right end of the bolt, the stress wave of the bolt propagates to the right end face of the bolt at 127 μs, and after reflection at the bottom, the stress wave propagates back along the positive Z-axis direction. Bolt stress wave travels 169 μs toward necking location, with some reflecting and some continuing to propagate. At 211 μs, the stress waves returned from the floor and bolt's necking position propagate in the Z-axis's positive direction. When it reaches the right end of the bolt, stress superposition occurs and the stress increases. The subsequent propagation process of stress waves is basically the same, but due to the loss of stress wave energy, the reflected stress waves continue to decrease.

A comprehensive comparison of Figures 8 and 9 shows that the deformation generated by bolt stretching explicitly affects stress wave progression within the bolt. This deformation results in the reflection phenomenon of stress waves, increasing energy loss. This indicates that the deformation generated by different stretching stages has a different degree of influence on the energy attenuation of the propagation process of the stress waves in the bolt. The degree of influence exerted by the stages of the bolt on the energy attenuation of the propagation process of the stress wave in the bolt varies. This finding corroborates the conjecture and law derived from experimental research. However, further research is needed to gain a more nuanced understanding of the quantitative evaluation of the relationship between bolt diameter and energy decay of stress wave detection.

3.3. Analysis of the Influence of Deformation on Stress Wave Propagation in Tensioning Bolts

Verify the energy attenuation law for stress waves in various stretching steps obtained from the test, the acceleration-time curves of five different strain moments at the left endpoint of the bolt were extracted with analyses, as shown in Fig. 10. The stress wave energy decay ratios for the acceleration-time curves at five different moments were calculated, and the results for different tensioning stages of the bolt were obtained, as shown in Table 1.

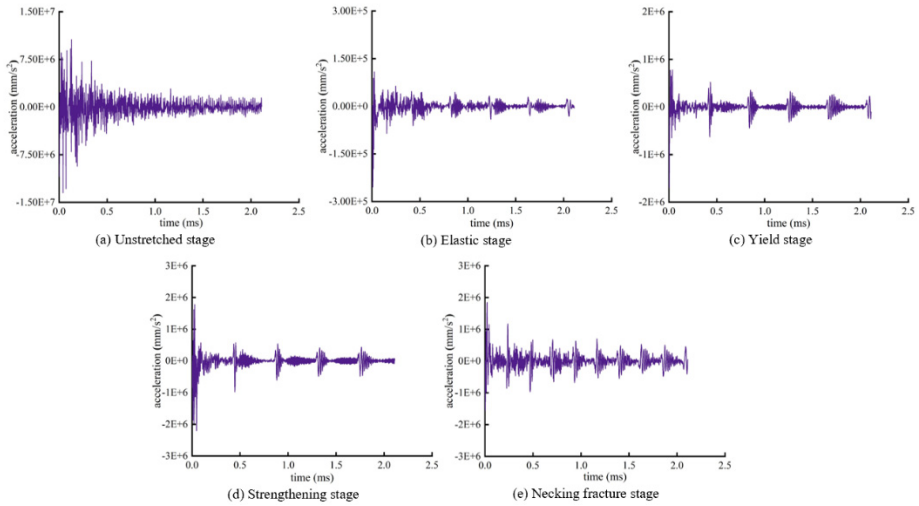

Fig 10. Stress wave acceleration-time curve of bolt at different stretching stages.

Table 1. Stress wave energy decay ratio results for bolt in various tension states.

Serial number	Stress wave energy decaying ratio (%)	
a	21.58	21.58
b	22.33	22.33
c	29.72	29.72
d	33.90	33.90
e	40.96	40.96

A comparison between stress wave energy decay results obtained from the numerical simulation and those obtained from laboratory tests showed a high degree of agreement. The numerical simulation results were in good agreement with the experimentally obtained laws.

4. Discussion

4.1. Verification Experiment of NDT Method For Bolt Based on Stress Wave Method

To verify the correctness of the law between the bolt deformation and energy decay from stress wave inside bolt, a validation experiment for NDT of bolt deformation due to stress wave technique is designed, and its feasibility is analyzed.

The validation experiment uses the stress wave technique to collect stress wave data from two bolts at different stages of deformation, as illustrated in Figure 11, for the randomly selected sampling points of the stress wave data at unused moments. To obtain the energy decay ratios within the stress wave in different moments, noise reduction and stress wave data analysis were performed. The diameter size for bolt constriction at that moment was determined based on the matching formula obtained previously. This diameter size was then compared with the minimum diameter of the bolt observed by the bolt condition monitoring system. The error rate between the two was calculated. Table 2 shows a summary of stress waves energy decay ratio for all sampling points.

As Figure 12 illustrates, the comparison of the calculation and monitoring results reveals an error curve with a detection error ranging from 0.12% to 4.11% and an average error of approximately 1.65%. The error in bolt diameter during the elastic stretching stage is minimal, whereas the strengthening stage exhibits fluctuations. When viewed in conjunction with the preceding analysis, these fluctuations can be attributed to the stress wave energy decay ratio during the oscillatory period. During bolt tensile deformation, this manifests as a brief period of heterogeneous deformation and a total elongation that differs from the total amount of elongation, resulting in a significant error. However, the error curve as a whole is smooth, and the error is small, which does not affect the accuracy of the detection results.

Table 2. Stress-wave detection energy decay ratio.

Specimen number	Stress wave energy attenuation ratio/%	Specimen number	Stress wave energy attenuation ratio/%
yz 1-1	23.64	yz 2-1	20.97
yz 1-2	28.31	yz 2-2	26.16
yz 1-3	32.55	yz 2-3	33.72
yz 1-4	37.42	yz 2-4	35.82
yz 1-5	39.65	yz 2-5	38.24
yz 1-6	42.58	yz 2-6	41.77

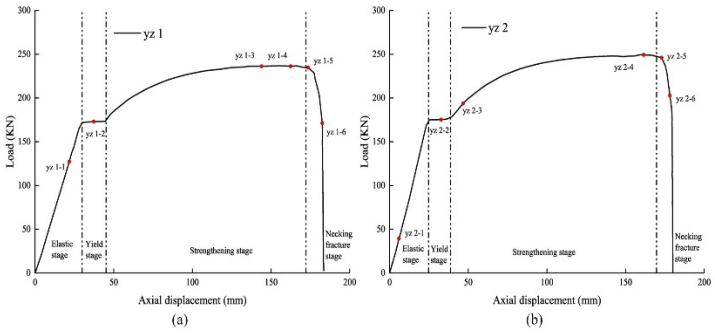

Fig 11. Stress-strain curve of verification experiment bolt.

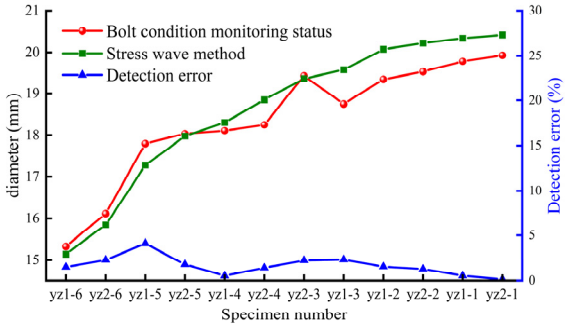

Fig 12. Comparison of detection results and error curve.

4.2. Verification Experiment of NDT Method for Bolt based on Stress Wave Method

The evaluation method proposed above, which uses the ratio of stress wave energy decay to evaluate bolt diameter at necking time, is combined with the necking ratios of bolt' diameters obtained from the monitoring of different deformation phases to propose the NDT evaluation criteria for the deformation state of bolt, as shown in Table 3.

Table 3. Evaluation criteria for NDT of bolt deformation under axial tensile stress.

Different stages of tension of the bolt	Necking ratio range (%)	Working status
Resiliency stage	98.57–100	The bolt continues to elongate under the action of tensile stress, the working load continues to increase, and the working condition is normal.
Yield stage	97.8–98.57	
Intensive stage	91.15–97.8	
Necking rupture stage	<91.15	The bolt has reached the tensile strength, and the local stress concentration occurs under the action of tensile stress, the working load is rapidly reduced, the working state is abnormal, and there are potential safety hazards.

From Table 3, it can be seen that the range of necking ratio of bolt in the elastic and yield stages is relatively small. In the strengthening stage, the necking ratio of bolt can reach a minimum of 91.15%. At this time, the diameter at the minimum diameter of the bolt body decreases by about 1.77 mm. At this time, the bolt has not yet reached its tensile strength and can still provide working resistance, and the working state is normal. After reaching the necking and fracture stage, the necking ratio of the bolt rapidly decreases, with a minimum reduction of 67.8%. At this time, the minimum diameter of the bolt is only 13mm, and the working load of the bolt rapidly decreases, resulting in abnormal working conditions and potential safety hazards.

5. Conclusion

This article focuses on the problem of NDT discrimination of plastic deformation status of bolt. Through comprehensive methods such as indoor experiments, numerical simulations, and experimental verification, the propagation characteristics of stress waves in different tensile stages of bolt are studied, the following conclusions can be drawn:

(1) The propagation law of stress waves in different tensile deformation stages of the bolt is revealed, and the energy decay ratio is proposed to characterize the degree of energy decay of stress waves. Initially, bolt deformation stress wave energy decay ratio is 20%. At the elastic and yield stages,

energy decay increases smoothly from 20% to 33%. During the strengthening phase, the energy decay ratio rises and falls along a trajectory that peaks at 33% and then remains at a relatively stable level. When the energy decay ratio reaches 35%, bolt enters the neck failure stage, then multiplies until the bolt is completely broken.

(2) Visualize the propagation process of stress waves in different tensile deformation stages of the bolt. The numerical simulation results demonstrate an attenuation phenomenon when stress waves propagate in the bolt, and the attenuation ability varies in different deformation stages.

(3) According to the propagation rules of stress waves at different stages of bolt tensile deformation, a method for evaluating the NDT of bolt deformation based on the stress wave method is proposed, along with an evaluation standard for the NDT of bolt deformation state. This method has been verified to have a small overall error, and it provides a theoretical basis for the research of NDT technology of bolt deformation state in-field support.

References

[1] Kang, H. et al. Forty years development and prospects of underground coal mining and strata control technologies in China. J. Min. Rock Strata Control Eng. 1, 7–39; 10.13532/ j. jmsce. cn10-1638/td.2019.02.002 (2019). (in Chinese)

[2] Kang, H. Sixty years development and prospects of rock bolting technology for underground coal mine roadways in China. J. China Univ. Min. Technol. 45, 1071–1081; 10. 132 47/j.cnki.jcumt.000583 (2016). (in Chinese)

[3] Yu, Z., Sun, X. & Liu, K. Loss characteristics of bolt pre-tightening force and surrounding rock control mechanism in coal roadway. Coal Eng. 55, 41–46; 10.11799/ce202303008 (2023). (in Chinese)

[4] Si, L., Lou, J., Yang, J. & Yuan, G. Deformation and stress characteristics of bolt bolt under axial impact. J. China Coal Soc. 47, 3645–3653; 10.13225/j.cnki.jccs.2022.0246 (2022). (in Chinese)

[5] Salita, D. S. & Polyakov, V. V. Acoustic emission during plastic deformation of Pb-Sn alloys. Phy. Mesomech. 23, 593–600; 10.1134/S1029959920060156 (2020).

[6] Ouyang, H. Research on plastic deformation of metal materials based on acoustic emission characteristic parameters [Master's Thesis]. Southwest Petroleum University (Chengdu, 2017). (in Chinese)

[7] Tian, S. Fracture monitoring of high strength bolts based on acoustic emission technology [Master's Thesis]. Dalian University of Technology (Dalian, 2021). (in Chinese)

[8] Ivanović, A. & Neilson, R. D. NDT testing of rock bolts for estimating total bolt length. Int. J. Rock Mech. Min. Sci. 64, 36–43; 10.1016/j.ijrmms.2013.08.017 (2013).

[9] Vrkljan, I., Szavits-Nossan, B. & Kovacevic, M. S. Nondestructive procedure for testing grouting quality of rockbolt bolts. In Proceedings of the 9th ISRM Congress. 1475–1478, (1999).

[10] Zhang, J. et al. Research on NDT testing method of GFRP bolts based on HHT signal analysis. Chin. J. Rock Mech. Eng. 40, 1460–1472; 10.13722/j.cnki.jrme.2020.0630 (2021). (in Chinese)

[11] Zhang, L. et al. Multiscale entropy analysis of NDT test signals of bolting defects of rock bolts. J. China Univ. Min. Technol. 50, 1077–1086; 10.13247/j.cnki.jcumt.001347 (2021). (in Chinese)

[12] Li, C. et al. Experimental study of the effect of axial load on stress wave characteristics of rock bolts using an NDT testing method. Sustainability 14, 9773; 10.3390/su14159773 (2022).

[13] Wang, Y., Zhang, K., Xiao, F., Cao, H. & Zhang, M. NDT testing method for bolt axial force based on vibration response characteristics of bolt components. J. Vibr. Shock 42, 119–126+146; 10.13465/j.cnki.jvs.2023.13.014 (2023). (in Chinese)

[14] Wang, M., Weng, S., Yu, X., Yan, J. & Yin, P. Structural damage identification based on time-varying modal mode shape of wavelet transformation. J. Vibr. Shock 40, 10–19; 10.13465/j.cnki.jvs.2021.16.002 (2021). (in Chinese)

[15] Hao, Y., Wu, Y., Zhang, K., Li, P. & Meng, Q. The analysis of vibration frequency parameter of rock bolt voltage system during axial force testing in the coal mine. J. Min. Saf. Eng. 39, 567–575; 10.13545/j.cnki.jmse.2021.0249 (2022). (in Chinese)

[16] Wu, F., Liu, M., A'BI, E., Wu, L. & Wu, T. State-of-the-art: NDT testing technology based on stress waves for the quality of rock bolt. Sci. Technol. Eng. 23, 5840–5852 (2023). (in Chinese)